ELSEVIER

International Journal of Mass Spectrometry and Ion Processes 163 (1997) 89–99

International Journal of Mass Spectrometry and Ion Processes

Stereoelectronic effects in phosphorus dichloride cation/pyridine complexes

Shuguang Ma[a], Philip Wong[a], R. Graham Cooks[a,*], Fabio C. Gozzo[b], Marcos N. Eberlin[b]

[a]*Department of Chemistry, Purdue University, West Lafayette, IN 47907-1393, USA*
[b]*State University of Campinas, Institute of Chemistry, CP 6154 Campinas, SP 13083-970, Brazil*

Received 3 October 1996; accepted 3 January 1997

Abstract

The kinetic method is applied to order the relative affinities of a group of substituted pyridines towards PCl_2^+ and to seek relationships with the affinities towards other cations. The absolute affinities are estimated with the aid of AM1 molecular orbital calculations while the PCl_2^+ affinity of pyridine itself is also estimated by ab initio calculations at MP2/6-31G(d,p)//6-31G(d,p) level to be 76.0 kcal mol^{-1}. The experiments employ the PCl_2^+-bound dimer of two pyridines generated via ion/molecule reactions between the mass-selected PCl_2^+ ion and a mixture of pyridines. The dimers, examined using MS^3 experiments, fragment exclusively to yield the pyridine/PCl_2^+ monomers and this is consistent with ab initio RHF/6-31G(d,p) and AM1 molecular orbital calculations which show a tetrahedral complex with a N–P–N angle of 129°. For meta- and para-substituted pyridines, there is an excellent linear correlation (slope 0.69) between the logarithm of the ratio of the two fragment ion abundances and the proton affinity of the corresponding substituted pyridine. Similar correlations are observed for other cations ($SiCl_3^+$, Cl^+, SF_3^+ and $SiCl^+$) and it is shown that both the number of degrees of freedom in the dimer and the cation affinity control this correlation.

Dimers comprising ortho-substituted pyridines show decreased affinities due to stereoelectronic interactions between the ortho-substituted alkyl group and the central PCl_2^+ cation. A set of gas phase stereoelectronic parameters (S^k) is determined and ordered as 2-MePy (–0.38) < 2,4-diMePy (–0.84) < 2,6-diMePy (–0.86) < 2,5-diMePy (–1.08) < 2,3-diMePy (–1.26). AM1 calculations show that the eclipsed conformation of 2-methylpyridine/PCl_2^+ adduct is more stable than the staggered conformation by approx. 3 kcal mol^{-1} and this is suggested to be due to a favorable agostic interaction between the hydrogen of the ortho methyl group and the central phosphorus atom. The most stable conformation is found when the two chlorines face the two hydrogens of the ortho methyl substituent in a "face-to-face" interaction. This novel type of interaction is also the reason for the relatively small magnitude of S^k, the stereoelectronic parameter, in 2,6-dimethylpyridine. The overall stereoelectronic effects of the ortho-substituent(s) on PCl_2^+ affinities indicate that steric effects dominate electronic effects in this system. The PCl_2^+ ion behaves similarly in its steric and agostic effects to SF_3^+ and very differently to $SiCl^+$ which displays uniquely strong agostic effects. © 1997 Elsevier Science B.V.

Keywords: Kinetic method; Stereoelectronic effects; Cation affinity; PCL_2^+; Thermochemistry; Agostic effects

* Corresponding author.

PII S0168-1176(97)00013-X

1. Introduction

Electron-deficient species are often highly reactive and the gas phase is an ideal environment in which to study their chemical and physical properties without perturbing influences such as solvation and ion-pairing. The present study of PCl_2^+ affinities, defined as the enthalpy change for the gas-phase reaction

$$B - PCl_2^+ \rightarrow B + PCl_2^+ \quad (1)$$

where B represents a Lewis base, continues a series of investigations which seek to provide thermochemical information useful for the interpretation and prediction of ion/molecule mechanisms and reactivities. Emphases are on steric and electronic effects due to ortho-substituent(s) in pyridines and PCl_2^+ is chosen as an accessible representative of divalent phosphorus cations.

The PCl_2 radical has received some attention [1]. It is known that the ground state is $^2B_1$ and the first low-lying excited state is $^2A_1$ [2]. The infrared [3] and ESR [4] spectra of the ground state PCl_2 radical show a bent geometry and C_{2v} symmetry. It is also reported that the ground state for PCl_2^+ ion is the $^1A_1$ state and the singlet–triplet energy separation ($^3B_1 - {}^1A_1$) is 2.12 eV while the singlet–singlet energy separation is 3.09 eV [1]. There are very few studies on the gas-phase ion chemistry and thermochemistry of the PCl_2^+ cation [5]. In this study of PCl_2^+ affinities of substituted pyridines, the kinetic method is used and the results are tested further against semi-empirical AM1 and ab initio calculations. The kinetic method is an approximate method for determining thermochemical properties through studies of the competitive dissociation of mass-selected cluster ions [6,7]. It has been widely used to measure proton affinities by the collision-induced dissociation or spontaneous metastable ion dissociation of proton-bound dimers comprising a compound of unknown proton affinity and a reference compound. The method has been used to determine proton affinities of various organic compounds [8–12] including free radicals [13], and it has been extended to the determination of electron affinities of PAHs and nitrobenzenes [14], NH_4^+ affinities of crown ethers [15], and the cation affinities of substituted pyridines using such cations as Cl^+ [16], CN^+ [17], $OCNCO^+$ [18], $SiCl^+$, $SiCl_3^+$ [19], and SF_3^+ [20], among other applications. The method is often sensitive to small thermochemical differences (below 1 kcal mol^{-1}) and is applicable to polar and non-volatile samples, even when they are not pure [7c].

The specific objectives of this study are (i) to order the relative PCl_2^+ affinities of a group of alkyl-substituted pyridines, (ii) to compare the PCl_2^+ bond strengths with those found previously for other cations, and (iii) to seek stereoelectronic effects which might arise for ortho-substituted alkyl pyridines and to relate them to stereoelectronic effects for other cations.

2. Experimental

All experiments were performed using a custom-built pentaquadrupole mass spectrometer [21]. The quadrupoles Q1, Q3, and Q5 operate in the r.f./d.c. mode (mass analysis) or in the r.f.-only mode (passing all ions), depending on the experiment of interest. Quadrupoles Q2 and Q4 operate only in the r.f.-only mode and are used as collision cells or simply to transmit ions.

Ion/molecule reactions (MS^2 experiments using mass-selected reagent ions) were performed using Q1 to mass-select the ion of interest generated in the ion source. After reaction in Q2 with the neutral reagent, Q3 and Q4 were both set in the r.f.-only mode to pass all the ions produced, and Q5 was then used to record the product spectrum. To perform MS^3 experiments, the ion/molecule reaction product formed in Q2 was mass-selected in Q3 and allowed to undergo collision-induced dissociation (CID) with argon in Q4, while Q5 was scanned to record the sequential product spectrum [22].

The ion PCl_2^+ was generated by 70 eV electron impact of phosphorus trichloride (Aldrich Chemical, Milwaukee, WI), which was introduced into the ion source via a Granville Phillips leak valve (Granville Phillips, Boulder, CO). The nominal sample pressure was typically 5×10^{-6} torr as monitored by a single ionization gauge located in the housing near Q5. The indicated pressure rose to 4×10^{-5} torr on addition of the pyridine mixture to Q2, and rose to 6×10^{-5} torr on addition of argon gas to Q4. The collision energy, given as the voltage difference between the ion source and the collision quadrupole, was typically near 0 eV for ion/molecule reactions and 10 eV for CID. The pyridines and phosphorus trichloride are commercially available and were used as-received. Mass-to-charge ratios are reported using the Thomson unit (1 Thomson (Th) = 1 atomic mass per unit positive charge) [23].

AM1 molecular orbital calculations [24] and ab initio calculations at the RHF/6-31G(d,p) and MP2/6-31G(d,p)//6-31G(d,p) level were carried out using SPARTAN 4.0 (SPARTAN version 4.0, Wavefunction Inc., 18401 Von Karma, Suite 370, Irvine, CA 92715). Zero-point energies (ZPE) were evaluated at the HF/6-31G(d,p) level and scaled by a factor of 0.89.

3. Results and discussion

Fig. 1 shows a typical MS^2 ion/molecule reaction product spectrum for the reactions between the mass-selected PCl_2^+ (101 Th) and a mixture of 3-methylpyridine (3-MePy) and pyridine (Py). Ion/molecule reactions lead to formation of products which include (i) protonated pyridines, PyH^+, 80 Th, and 3-$MePyH^+$, 94 Th, (ii) PCl_2^+ adducts, $PyPCl_2^+$, 180 Th and 3-$MePyPCl_2^+$, 194 Th, (iii) H^+-bound dimers, PyH^+Py, 159 Th, PyH^+3-MePy, 173 Th, and 3-$MePyH^+$3-MePy, 187 Th, and (iv) PCl_2^+-bound dimers, $PyPCl_2^+Py$, 259 Th, $PyPCl_2^+$3-MePy, 273 Th, and 3-$MePyPCl_2^+$3-MePy, 287 Th. The protonated pyridines and the proton-bound dimers are most likely formed by an initial charge–exchange reaction between the mass-selected reagent ion and a pyridine and subsequent proton transfer and association reactions.

The structure of PCl_2^+ cation, calculated ab initio at the RHF/6-31 G(d,p) level, is shown in

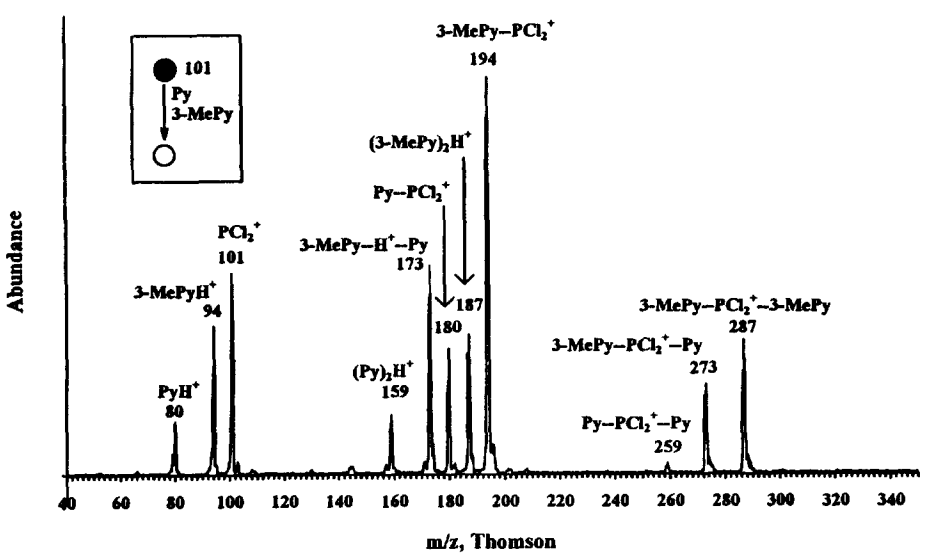

Fig. 1. Reaction product spectrum showing ion/molecule reactions of PCl_2^+ (101 Th) with a mixture of pyridine (Py) and 3-methylpyridine (3-MePy).

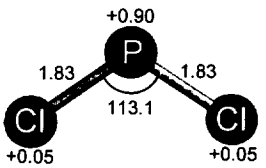

Fig. 2. The geometry of PCl_2^+ from ab initio calculations at RHF/6-31G(d,p) level.

Fig. 2. The positive charge is mainly localized on the phosphorus atom (+0.90) while each chlorine atom has a charge density of only +0.05; a P–Cl bond length of 1.83 Å and a Cl–P–Cl angle of 113.1° were calculated. The high charge density on the phosphorus atom suggests that this should be the favored bonding site to pyridines. The structure of the dimer, Py–PCl_2^+–Py, obtained by AM1 calculations is shown in Fig. 3. The dimer is symmetrical with respect to the nitrogen atoms of the two pyridines bound to the central phosphorus atom, with an N–P–N bond angle of 129.0° and an N–P bond length of 1.72 Å. The P–Cl bonds are weakened (length increased by 0.11 Å) with respect to those in the free cation.

The unsymmetrical PCl_2^+-bound dimer, 3-MePyPCl_2^+Py, 273 Th, mass-selected in Q3 and

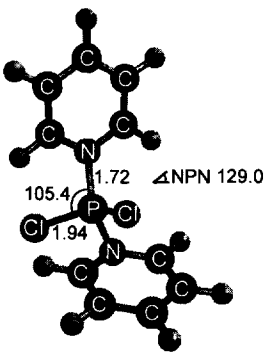

Fig. 3. Structure of lowest energy form of the Py[PCl_2^+]Py dimer.

fragmented by CID with argon in Q4 under mild conditions (collision energy 10 eV and pressure 6×10^{-5} torr), fragmented to yield the two PCl_2^+-bound monomers, PyPCl_2^+, 180 Th, and 3MePyPCl_2^+, 194 Th, as shown in Fig. 4. Comparison of the relative abundances of these two fragments indicates that 3-MePy has a higher affinity for PCl_2^+ than that of pyridine itself, which is the same order as their proton affinities.

From the kinetic method, if entropy effects are negligible and reverse activation energies are zero or cancel, the logarithm of the relative abundances of the two fragment ions is directly

Table 1
PCl_2^+ affinities and proton affinities of pyridines

Entry	Pyridines	Py_1:Py_2[a]	$\ln\{[Py_1(PCl_2^+)]/[Py(PCl_2^+)]\}$[b]	Proton affinity[c]/ kcal mol^{-1}	AM1 PCl_2^+ affinity/kcal mol^{-1}
1	Py		0	220.4	67.5
2	3-MePy	2:1	1.74	222.8	69.3
3	4-MePy	3:1	2.0	223.7	70.8
4	3-EtPy	4:2	1.87	223.9	69.8
5	4-EtPy	5:2	2.75	224.6	71.2
6	3,5-diMePy	6:3	3.64	225.5	70.9
7	3,4-diMePy	8:3	3.99	226.2	73.4
8	2-MePy	10:1	1.79	223.7	67.4[d]
9	2,5-diMePy	11:3	2.81	226.2	69.0[d]
10	2,3-diMePy	12:3	2.63	226.2	68.1[d]
11	2,4-diMePy	13:3	3.53	226.9	70.3[d]
12	2,6-diMePy	14:3	3.65	227.1	66.6[d]

[a] The entry number of the pyridine forming the PCl_2^+-bound dimer used to estimate the PCl_2^+ affinity.

[b] Experimental results.

[c] Proton affinities are taken from D.H. Aue, M.T. Bowers, in: M.T. Bowers (Ed.), Gas Phase Ion Chemistry, Vol. 2, Academic Press, New York, 1979. This older set of values is used in preference to others because it is more internally consistent and it facilitates comparison of the present data with those for pyridine binding to other cations.

[d] The affinity value is calculated based on the most stable conformation.

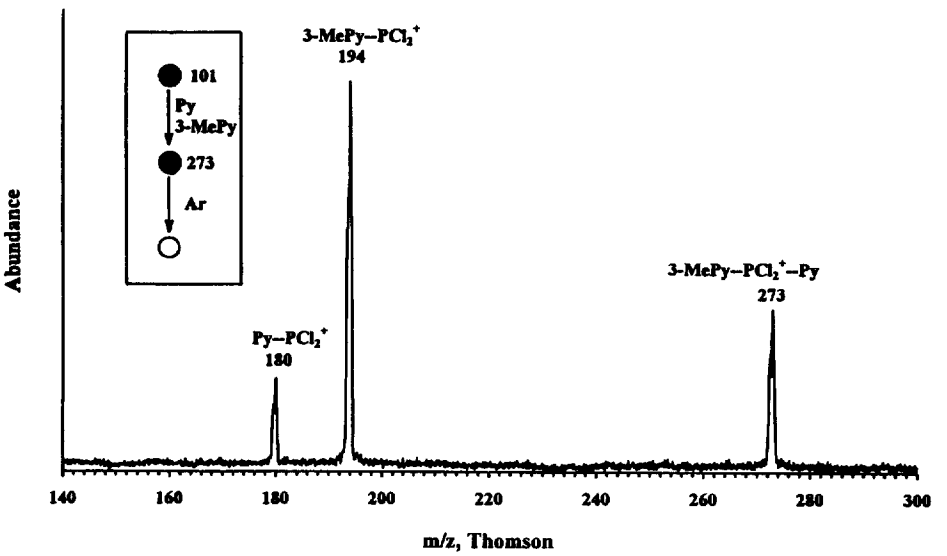

Fig. 4. Sequential product (MS^3) spectrum showing the two fragments generated from the mixed dimeric adduct (273 Th).

related to the difference in the PCl_2^+ affinities of the two pyridines

$$\ln\frac{[Py_1PCl_2^+]}{[Py_2PCl_2^+]}=\frac{\Delta(PCl_2^+\text{ affinity})}{RT_{\text{eff}}} \quad (2)$$

In this equation, $[Py_1PCl_2^+]$ and $[Py_2PCl_2^+]$ are the abundances of the two PCl_2^+-bound pyridine monomers, $\Delta(PCl_2^+$affinity) is the PCl_2^+ affinity difference between the two pyridines, R is the gas constant, and T_{eff} is the effective temperature of the activated dimer and is related to the energy of the dimer in excess of the critical energy for its dissociation divided by the number of degrees of freedom [25]. The application of this relationship is limited by the lack of independently known PCl_2^+ affinity values and the difficulty in measuring experimentally the effective temperature. However, it is possible to order the PCl_2^+ affinities using the quantity $\ln([Py_1PCl_2^+]/[Py_2PCl_2^+])$ which is directly proportional to the difference in the PCl_2^+ affinities of the two pyridines as shown in Eq. (2). The results are summarized in Table 1. The order of PCl_2^+ affinities of a series of substituted pyridines is: Py < 3-MePy < 3-EtPy < 4-MePy < 4-EtPy < 3,5-diMePy < 3,4-diMePy. If the same electronic effects that influence proton affinities also affect PCl_2^+ affinities, a linear relationship is expected between $\ln(k_1/k_2)$, the logarithm of the relative dissociation rates, and the PA values of meta- or para-substituted pyridines. As shown in Fig. 5, such a linear correlation indeed exists ($r^2 = 0.97$) and it is described in kcal mol^{-1} by

$$\ln(k_1/k_2)=0.69\text{PA}-152.22 \quad (3)$$

This result is consistent with those for other cations, the affinities of which correlate linearly with the proton affinities of meta- and para-substituted pyridines [16–20]. An excellent linear relationship between the free energy change upon iodine cation bonding and the gas phase basicities of a series of meta- and para-substituted pyridines in the gas phase has also been reported using equilibrium measurements of I^+ transfer between two pyridines [26]. The implications of these correlations are discussed below.

Since no PCl_2^+ affinities of pyridines have been reported, AM1 molecular orbital calculations which have proved useful in estimating other ionic affinities [27] are used to estimate the PCl_2^+ affinities. These results are also listed in Table 1. The PCl_2^+ affinity of pyridine itself is

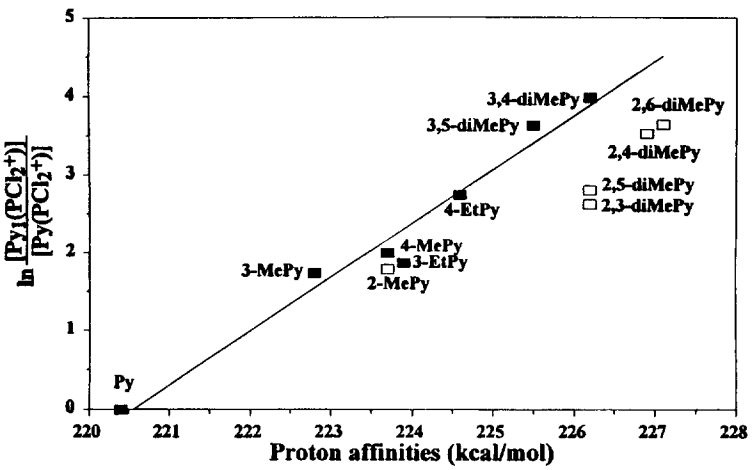

Fig. 5. Linear correlation between $\ln\{[Py_1(PCl_2^+)]/[Py(PCl_2^+)]\}$ and the corresponding proton affinities. Open symbols represent ortho-substituted pyridines which do not correlate due to steric effects.

also estimated to be 76.0 kcal mol^{-1} by ab initio calculations at MP2/6-31G(d,p)//6-31G(d,p) level, which is sufficiently close to the value of 67.5 kcal mol^{-1} from AM1 molecular orbital calculations to allow the use of AM1 values for the relative affinities of the substituted pyridines. A linear correlation exists between the quantity $\ln([Py_1PCl_2^+]/[Py_2PCl_2^+])$ and the PCl_2^+ affinities determined from AM1 calculations for unhindered pyridines, as is evident in Fig. 6. From Eq. (2), the slope of this correlation is equal to $1/RT_{eff}$, and therefore, T_{eff} is calculated to be 782 ± 80 K, where the uncertainty does not include systematic errors in the AM1 results. A similar approach was used to investigate Cl^+ [16] and SF_3^+

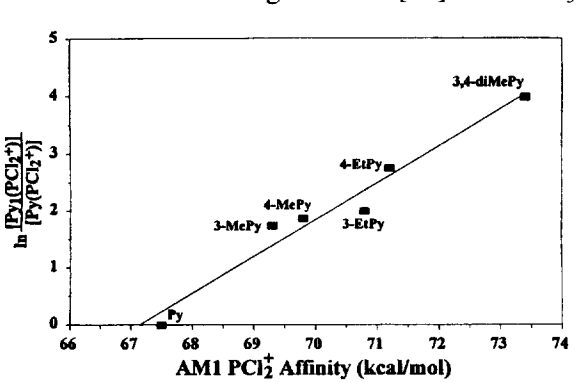

Fig. 6. Linear correlation between $\ln\{[Py_1(PCl_2^+)]/[Py(PCl_2^+)]\}$ and the corresponding calculated AM1 PCl_2^+ affinities.

affinities [20]. Good correlations were also observed between the AM1 and the experimental Cl^+ and SF_3^+ affinities for the unhindered pyridines. From the slope of the correlation lines in these cases, the effective temperatures were calculated to be 555 K and 595 K, respectively. However, an accurate knowledge of the effective temperature is not required to calculate the affinities. For example, errors in this temperature of even ± 200 K correspond to changes in affinities of only ± 1.2 kcal mol^{-1}.

As shown in Fig. 5, the correlation of the logarithm of the ion abundance ratio with proton affinity is generally excellent for meta- and para-substituted pyridines, but poor for the ortho-substituted pyridines. Lower than expected cation affinities for pyridines with ortho substituent(s) are most readily attributed to steric hindrance between the central cation and the ortho-group(s) as shown below, but electronic effects also contribute. The deviation from the regression line due to the combination of steric and electronic effects of the ortho group is defined as the gas-phase stereoelectronic parameter (S^k) [16].

Steric effects do not exist in proton-bound dimers due to the very small size of the proton. For example, 2-MePy and 4-MePy have the same

Table 2
Comparison of steric parameters (S^k) for ortho-substituted pyridines

Pyridine	S^k (PCl_2^+)[a]	S^k (Cl^+)[b]	S^k ($SiCl_3^+$)[c]	S^k ($SiCl^+$)[c]	S^k (SF_3^+)[d]
2-MePy	–0.38	–0.43	–0.47	0.15	–1.09
2,5-diMePy	–1.08	–	–0.32	0.78	–2.25
2,3-diMePy	–1.26	–0.64	–0.22	0.55	–2.15
2,4-diMePy	–0.84	–	–0.71	–0.17	–2.4
2,6-diMePy	–0.86	–1.6	–0.94	1.62	–1.11

[a] S^k value is obtained from the deviation of experimental data from the regression line. Uncertainties are less than ± 0.1.
[b] S^k value is obtained from Ref. [16].
[c] S^k value is obtained from Ref. [19].
[d] S^k value is obtained from Ref. [20].

proton affinities, both of which have affinities higher than that of 3-MePy (Table 1). This can be understood by the fact that ortho- and para-methyl groups have similar electronic effects but they are higher than those of meta-methyl groups. In the case of PCl_2^+, the affinity order is different: 2-MePy < 3-MePy < 4-MePy. The decrease in PCl_2^+ affinity of 2-MePy is clearly due to steric hindrance arising from the ortho-substituent. The gas-phase stereoelectronic parameters (S^k) measured by the deviation of the experimental data from the regression line are 2-MePy (–0.38) < 2,4-diMePy (–0.84) < 2,6-diMePy (–0.86) < 2,5-diMePy (–1.08) < 2,3-diMePy (–1.26) (Table 2).

Although the overall effects of ortho-substitution correspond to steric hinderance, auxiliary bonding which offsets the steric effects is indicated by a detailed examination of the experimental results and those of AM1 calculations. It is instructive to consider the monomer, 2-MePy–PCl_2^+, for which the lowest affinity (highest heat of formation) corresponds to the staggered conformation **a** while the eclipsed conformation **b** (more crowded than staggered conformation **a**) is calculated to be more stable by 2.7 kcal mol^{-1}. Structure **a** is unstable and collapses into structure **b** during free optimization. This unexpected result indicates an opposing effect which increases the cation affinity in the more crowded eclipsed conformation. Note that the hydrogen in the eclipsed conformation **b** is closer to the central phosphorus than that in the staggered conformation **a**; therefore, a stronger interaction between the hydrogen of the methyl group and the phosphorus atom is possible and a higher affinity (lower heat of formation) results (Fig. 7). Such a three-center two-electron interaction is known as gas-phase agostic bonding [19].

Agostic bonding has been observed in many organometallic compounds in which a carbon–hydrogen group interacts with a transition metal center to form a three-center two-electron bond (C–H → M) [28]. This is similar to the familiar bridging hydrogen systems which occur in B–H → B, M–H → M, and B–H → M groups. Agostic bonding in the gas phase was first observed in a study of the $SiCl^+$ affinities of a series of alkyl-substituted pyridines [19]. Higher than expected $SiCl^+$ affinities were observed for ortho-substituted pyridines due to the auxiliary (agostic) bonding between the hydrogen in the ortho-methyl group and the central silicon atom in the form of a three-center two-electron bond (C–H → Si) [19]. The availability of vacant d-orbitals on the silicon of the $SiCl^+$ cation and the sterically favorable orientation of the ortho-substituted methyl group, promotes intramolecular auxiliary bonding between the hydrogen in the methyl group and the central silicon atom. This auxiliary bonding stabilizes the Si–N bond and, therefore, increases the affinity of the ortho-substituted pyridines toward the $SiCl^+$ cation. More recently, Abboud and co-workers reported a similar phenomenon showing the existence of a novel three-center delocalized

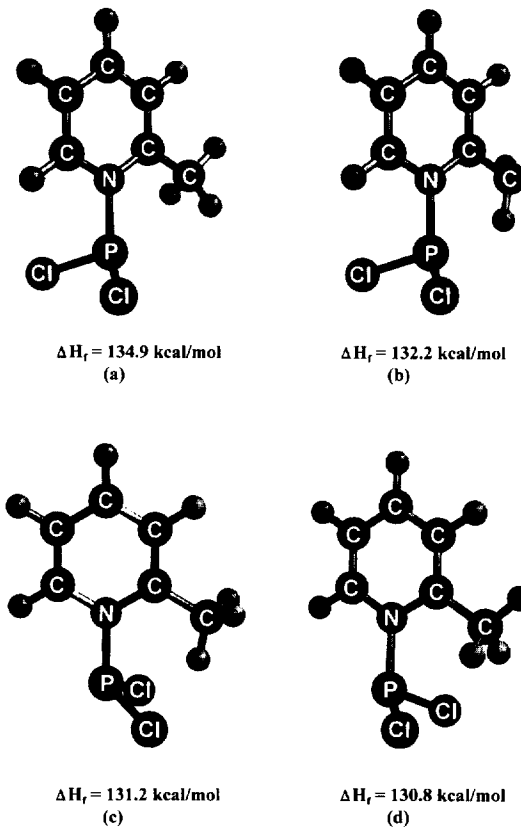

Fig. 7. Conformations and enthalpies of the PCl_2^+/2-methylpyridine adduct: (a) staggered conformation, (b) eclipsed conformation, (c) eclipsed conformation with interaction with the two chlorines, (d) staggered conformation with "face-to-face" interactions. The lower energy of (b) than (a) by 2.7 kcal mol^{-1} is evidence for agostic bonding.

P–H–P bond in protonated P_4. The incoming proton inserts between two phosphorus atoms to replace the initial P–P bond by a three-center two-electron bond with similar characteristics to those found in diborane [29].

Note that agostic bonding is also evident in conformation **c** (Fig. 7) of the PCl_2^+/2-methylpyridine adduct, in spite of the fact that the methyl hydrogen is much closer to the two chlorine atoms. In fact, the calculations show that the most stable conformation is that in which the two hydrogens in the staggered methyl group face the two chlorines, as shown in conformation **d**. "Face-to-face" dipolar interactions compete with the steric effects and result in increasing affinity in **d**.

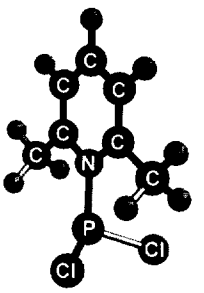

Fig. 8. The most stable conformation of the adduct PCl_2^+/2,6-dimethylpyridine. Note the "face-to-face" orientations of the two Cl and H atoms.

This discussion of bonding in the mono-substituted pyridine allows one to understand the results for the case of 2,6-dimethylpyridine. If one only considers steric effects, 2,6-dimethyl-pyridine containing two ortho-substituents should have the largest steric parameter among the dimethyl series as is the case in the corresponding Cl^+ [16], $OCNCO^+$ [18], and $SiCl_3^+$ [19] dimers. However, the S^k value for 2,6-diMePy is even smaller than that for either 2,5-diMePy or 2,3-diMePy, which indicates the presence of an opposing effect. AM1 calculations show that the most stable conformation of the 2,6-diMePy/PCl_2^+ complex is a novel conformation in which one methyl group is directed "face-to-face" with the two chlorines while the other methyl group has a staggered conformation (Fig. 8). The smaller stereoelectronic parameter for 2,6-diMePy is therefore ascribed to the buttressing effect of the methyl group which shortens the N–P bond and increases the "face-to-face" interactions between the two hydrogens and chlorines. However, overall lower than expected affinities of ortho-substituted pyridines found in the case of PCl_2^+ indicate that the steric effects in the dimers are greater than the electronic effects.

4. Comparisons with other cations

It is possible to compare the PCl_2^+ data with those for previously studied cations having different bonding atoms and different sizes, in

order to develop an understanding of the relationship between the affinities of a single set of bases (substituted pyridines) for different cations. Remarkably good correlations are observed between the logarithm of the fragmentation ion abundance ratio, which from Eq. (2) is proportional to the cation affinity, and proton affinities for the meta- and para-substituted pyridines. This is the case for each cation studied and Fig. 5 represents just one typical example. These correlations imply that simple electrostatic effects dominate all these Lewis acid/base interactions. From Eq. (2), the slope of the linear correlation depends both on the cation affinity of the pyridine and on the effective temperature of the cation-bound dimer. Hence, the underlying correlation of cation affinity and proton affinity should be examined by a plot of $RT_{\text{eff}}[\ln(k_1/k_2)]$ vs. PA. The effective temperature (T_{eff}) is dependent on the quality of the AM1 calculations and on the exact conditions used for collisional activation, making comparisons between cations difficult. However, it can be expressed as the total non-fixed energy of the activated dimer (namely the internal energy of the ion minus the critical energy for fragmentation, $(\epsilon - \epsilon_0)$ divided by the number of degrees of freedom in the cluster [25]. Hence, a degree of freedom effect is expected. The slopes of the plots of the logarithm of the fragment ion abundance ratio vs. PA fall in the order $SiCl_3^+$ (0.86) > Cl^+ (0.83) > PCl_2^+ (0.69) > SF_3^+ (0.62) > $SiCl^+$ (0.55), while ab initio calculations at the MP2/6-31G(d,p)//6-31G(d,p) level show the cation affinities to pyridine itself to be 88.47, 201.05, 76.03, 51.61 and 65.71 kcal mol^{-1}, respectively. The differences between these values clearly demonstrate the degrees of freedom effect in the dissociation of the activated dimer cluster. For example, the Cl^+ affinity of pyridine is the largest among the cations studied, but it does not give the largest slope because of the relatively small number of degrees of freedom in the dimer.

Table 2 compares the stereoelectronic parameters (S^k) for PCl_2^+ with those for other cations studied previously. Significant steric effects (negative values) are observed for all cation/*o*-substituted pyridine combinations except for $SiCl^+$, which shows strong agostic effects (positive S^k values). Comparison of the stereoelectronic parameter for 2-MePy in the Cl^+-bound dimer (S^k–0.43), $SiCl_3^+$-bound dimer (S^k–0.47), SF_3^+-bound dimer (S^k–1.09), and PCl_2^+-bound dimer (S^k–0.38) clearly demonstrates that the SF_3^+ system has the largest steric effect, probably due to the lone pair of electrons on the sulfur atom which causes an approximately square-pyramidal structure for the dimer and therefore more steric crowding when an ortho-substituent is present on the pyridine [20]. This is also evident from ab initio calculations which show an N–S–N bond angle of 98.4° in SF_3^+-bound dimeric ion, while a much larger bond angle of N–P–N of 129.0° and a reduced steric effect is observed in PCl_2^+-bound dimer.

Agostic effects are evident in PCl_2^+/*o*-substituted pyridine complexes and their existence is supported by the calculations. The overall negative S^k values for all the PCl_2^+ cases (Table 2) indicate that the steric effects are stronger than the agostic effects. Similar results are obtained for the SF_3^+ system. However, the positive S^k values for the ortho-substituted pyridines in the $SiCl^+$ case indicate strong agostic effects which overcome the steric effects and lead to a net increase in the $SiCl^+$ affinities. The relatively weak agostic effects observed in the PCl_2^+ and SF_3^+ systems are probably due to the large steric bulk of the PCl_2 and SF_3 groups compared to the SiCl group and the long N–P and N–S bonds, which result in a large separation between the hydrogen of the ortho-methyl group and the central phosphorus and sulfur atoms, thus reducing the agostic interactions.

5. Conclusions

The cluster ions, PCl_2^+-bound dimers of neutral pyridines, can be generated via ion/molecule

reactions in a pentaquadrupole mass spectrometer. The kinetic method is applied to measure the relative PCl_2^+ affinities, and semi-empirical AM1 molecular orbital calculations are used to estimate the absolute affinities. The PCl_2^+ affinity of pyridine is 67.5 kcal mol^{-1} from AM1 calculations while ab initio calculations give a value of 76 kcal mol^{-1}. There is an excellent linear correlation between $\ln([Py_1PCl_2^+]/[PyPCl_2^+])$ and the proton affinities of the unhindered pyridines. The slope of this correlation is compared with analogous data for other cations. Comparisons of the entire data set are made with the cation affinities derived from ab initio calculations and they reveal that both the magnitude of the cation affinity and the number of degrees of freedom in the cluster cation affect the relative rates of competitive fragmentation of the dimer to give the two cationized monomers. Two opposing effects, steric and agostic interactions, affect the PCl_2^+ affinities of ortho-substituted pyridines. The presence of agostic bonding is supported by calculations showing that the eclipsed conformation of the 2-methylpyridine/PCl_2^+ adduct is more stable than the staggered form. Bonding between the hydrogen of the ortho-methyl group and the central phosphorus atom and hydrogen/chlorine bonding (''face-to-face'' interaction) are suggested from AM1 calculations. Although the differences in the energies of the various product conformations are not large, the most stable conformation should still have a significant effect on the thermochemical properties of the ion. The fact that the calculations rationalize the experimental data supports these conclusions. The PCl_2^+ ion behaves similarly in its steric and agostic effects to SF_3^+ and very differently to $SiCl^+$, which isplays uniquely strong agostic effects. The face-to-face binding, however, is unique to PCl_2^+.

Acknowledgements

The work at Purdue was supported by the National Science Foundation, CHE 92-23791. The research at UNICAMP was supported by the Research Support Foundation of the State of São Paulo (FAPESP) and the Brazilian National Research Council (CNPq).

References

[1] (a) J.L. Brum, J.W. Hudgens, J. Phys. Chem. 98 (1994) 5587. (b) G.L Gutsev, Chem. Phys. 179 (1994) 325.
[2] L. Latifzadeh, K. Balasubramanian, Chem. Phys. Lett. 241 (1995) 13.
[3] L. Andrews, D.L. Frederick, J. Phys. Chem. 73 (1969) 2774.
[4] L. Bonazzola, J.P. Michaut, J. Roncin, J. Chem. Phys. 75 (1981) 4829.
[5] (a) M. Veljković, O. Nešković, M. Miletić, J. Čomor, K.F. Zmbov, Adv. Mass Spectrom. 10B (1985) 1149. (b) T. Özgen, Int. J. Mass Spectrom. Ion Phys. 48 (1983) 427.
[6] (a) R.G. Cooks, T.L. Kruger, J. Am. Chem. Soc. 99 (1979) 1279. (b) S.A. McLuckey, D. Cameron and R.G. Cooks, J. Am. Chem. Soc. 103 (1981) 1313.
[7] (a) R.G. Cooks, J.S. Patrick, T. Kotiaho, S.A. McLuckey, Mass Spectrom. Rev. 13 (1994) 287. (b) L.G. Wright, S.A. McLuckey, R.G. Cooks and K.V. Wood, Int. J. Mass Spectrom. Ion Processes 42 (1982) 115. (c) J.S. Brodbelt and R.G. Cooks, Talanta 36 (1989) 255.
[8] B.D. Nourse, R.G. Cooks, Int. J. Mass Spectrom. Ion Processes 106 (1991) 249.
[9] S.T. Graul, M.E. Schnute, R.R. Squires, Int. J. Mass Spectrom. Ion Processes 96 (1990) 181.
[10] (a) T.K. Majumdar, F. Clairet, J.-C Tabet, R.G. Cooks, J. Am. Chem. Soc. 114 (1992) 2897. (b) M.J. Hass and A.G. Harrison, Int J. Mass Spectrom. Ion Processes 124 (1993) 115.
[11] (a) S.A. McLuckey, R.G. Cooks, J.E. Fulford, Int. J. Mass Spectrom. Ion Processes 52 (1983) 165. (b) X. Li and A.G. Harrison, Org. Mass Spectrom. 28 (1993) 366.
[12] (a) Z. Wu, C. Fenselau, Rapid Commun. Mass Spectrom. 6 (1992) 403. (b) Z. Wu and C. Fenselau, Rapid Commun. Mass Spectrom. 8 (1994) 777. (c) G. Bojesen and T. Breindahl, J. Chem. Soc. Perkin Trans. 2 (1994) 1029.
[13] (a) S.H. Hoke II, S.S. Yang, R.G. Cooks, D.A. Hrovat, W.T. Borden, J. Am. Chem. Soc. 116 (1994) 4888. (b) G. Chen, N. Kasthurikrishnan and R.G. Cooks, Int. J. Mass Spectrom. Ion Processes 151 (1995) 69.
[14] (a) D.J. Burinsky, E.K. Fukuda, J.E. Campana, J. Am. Chem. Soc. 106 (1984) 2770. (b) G. Chen and R.G. Cooks, J. Mass Spectrom. 30 (1995) 1167.
[15] (a) C.C. Liou, J.S. Brodbelt, J. Am. Chem. Soc. 114 (1992) 6761. (b) H.-F. Wu and J.S. Brodbelt, J. Am. Soc. Mass Spectrom. 4 (1993) 718.
[16] M.N. Eberlin, T. Kotiaho, B. Shay, S.S. Yang, R.G. Cooks, J. Am. Chem. Soc. 116 (1994) 2457.
[17] S.S. Yang, O. Bortolini, A. Steinmetz, R.G. Cooks, J. Mass Spectrom. 30 (1995) 184.

[18] S.S. Yang, G. Chen, S. Ma, R.G. Cooks, F.C. Gozzo, M.N. Eberlin, J. Mass Spectrom. 30 (1995) 807.
[19] S.S. Yang, P. Wong, S. Ma, R.G. Cooks, J. Am. Soc. Mass Spectrom. 7 (1996) 198.
[20] P. Wong, S. Ma, S.S. Yang, R.G. Cooks, F.C. Gozzo, M.N. Eberlin, J. Am. Soc. Mass Spectrom. 8 (1997) 68.
[21] J.C. Schwarz, K.L. Schey, R.G. Cooks, Int. J. Mass Spectrom. Ion Processes 101 (1990) 1.
[22] (a) J.C. Schwarz, A.P. Wade, C.G. Enke, R.G. Cooks, Anal. Chem. 62 (1990) 1809. (b) R.G. Cooks, J. Amy, M. Bier, J.C. Schwarz and K.L. Schey, Adv. Mass Spectrom. 11 (1989) 33. (c) V.F. Juliano, F.C. Gozzo, M.N. Eberlin, C. Kascheres and C.L. Lago, Anal. Chem. 68 (1996) 1328.
[23] R.G. Cooks, A.L. Rockwood, Rapid Commun. Mass Spectrom. 5 (1991) 93.
[24] M.J.S. Dewar, E.G. Zoebisch, E.F. Healy, J.J.P. Stewart, J. Am. Chem. Soc. 107 (1985) 3902.
[25] (a) H.-N. Lee, J.L. Beauchamp, to be published in J. Phys. Chem. (b) S.L. Craig, M. Zhong, B. Choo and J.I. Brauman, submitted to J. Phys. Chem.
[26] J.-L.M. Abboud, R. Notario, L. Santos, C. López-Mardomingo, J. Am. Chem. Soc. 111 (1989) 8960.
[27] (a) I. Sethson, D. Johnels, T. Lejon, U. Edlund, B. Wind, A. Sygula, P.W. Rabideau, J. Am. Chem. Soc. 114 (1992) 953. (b) M.J.S. Dewar, J.C. Hwang and D.R. Kuhn, J. Am. Chem. Soc. 113 (1991) 735.
[28] (a) M. Brookhart, M.L.H. Green, J. Organomet. Chem. 250 (1983) 395. (b) M.L.H. Green, Pure Appl. Chem. 56 (1984) 47. (c) M. Brookhart, M.L.H. Green and L.-L. Wong, in S.J. Lippard (Ed), Progress in Organic Chemistry, Vol. 36, Wiley, New York, 1988, p. 1. (d) R.B. King (Ed), Encyclopedia of Inorganic Chemistry, Vol. 1, Wiley, New York, 1994, p. 35.
[29] J.-L.M. Abboud, M. Herreros, R. Notario, M. Esseffar, O. Mó, M. Yáñez, J. Am. Chem. Soc. 118 (1996) 1126.